This article was downloaded by: [Renmin University of China]
On: 13 October 2013, At: 10:33
Publisher: Taylor & Francis
Informa Ltd Registered in England and Wales Registered Number: 1072954 Registered office: Mortimer House, 37-41 Mortimer Street, London W1T 3JH, UK

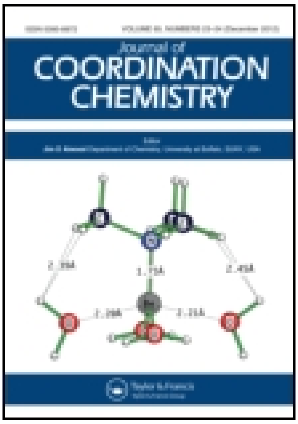

Journal of Coordination Chemistry
Publication details, including instructions for authors and subscription information:
http://www.tandfonline.com/loi/gcoo20

Kinetics and mechanism of chelating reaction between chitosan derivatives with Ca(II)

Ping Ding [a], Gui-Yin Li [b], Cui-Mei Chen [c] & Ke-Long Huang [d]
[a] School of Public Health, Central South University, Hunan 410078, China
[b] Biomedical Engineering Research Centre of Guilin University of Electronic Technology, Guilin, Guangxi 541014, China
[c] YUELU Center for Disease Control and Prevention, Changsha, Hunan 410013, China
[d] College of Chemistry and Chemical Engineering, Central South University, Hunan 410083, China

Published online: 08 Apr 2011.

To cite this article: Ping Ding, Gui-Yin Li, Cui-Mei Chen & Ke-Long Huang (2011) Kinetics and mechanism of chelating reaction between chitosan derivatives with Ca(II), Journal of Coordination Chemistry, 64:8, 1333-1343, DOI: 10.1080/00958972.2011.568615

To link to this article: http://dx.doi.org/10.1080/00958972.2011.568615

PLEASE SCROLL DOWN FOR ARTICLE

Taylor & Francis makes every effort to ensure the accuracy of all the information (the "Content") contained in the publications on our platform. However, Taylor & Francis, our agents, and our licensors make no representations or warranties whatsoever as to the accuracy, completeness, or suitability for any purpose of the Content. Any opinions and views expressed in this publication are the opinions and views of the authors, and are not the views of or endorsed by Taylor & Francis. The accuracy of the Content should not be relied upon and should be independently verified with primary sources of information. Taylor and Francis shall not be liable for any losses, actions, claims, proceedings, demands, costs, expenses, damages, and other liabilities whatsoever or howsoever caused arising directly or indirectly in connection with, in relation to or arising out of the use of the Content.

This article may be used for research, teaching, and private study purposes. Any substantial or systematic reproduction, redistribution, reselling, loan, sub-licensing, systematic supply, or distribution in any form to anyone is expressly forbidden. Terms &

Journal of Coordination Chemistry
Vol. 64, No. 8, 20 April 2011, 1333–1343

Kinetics and mechanism of chelating reaction between chitosan derivatives with Ca(II)

PING DING†*, GUI-YIN LI‡, CUI-MEI CHEN§ and KE-LONG HUANG¶

†School of Public Health, Central South University, Hunan 410078, China
‡Biomedical Engineering Research Centre of Guilin University of Electronic Technology, Guilin, Guangxi 541014, China
§YUELU Center for Disease Control and Prevention, Changsha, Hunan 410013, China
¶College of Chemistry and Chemical Engineering, Central South University, Hunan 410083, China

(*Received 31 January 2010; in final form 9 February 2011*)

Chitosan derivatives, such as chitosan alpha-ketoglutaric acid (KCTS) and hydroxamated chitosan alpha-ketoglutaric acid (HKCTS), are prepared and their coordination behavior toward Ca(II) was studied. The adsorption isotherms were correlated by $\mathrm{d}c/\mathrm{d}t = -kc^n$ at 20°C, 30°C, 40°C, 50°C, and 60°C. By linear correlation, the shapes of the isotherm curves were similar to the kinetic function of $1/c = kt$ and the rate equation was $\mathrm{d}c/\mathrm{d}t = -kc^2$; the activation energies were 13.31 and 14.76 $\mathrm{kJ\,mol^{-1}}$ for KCTS and HKCTS, respectively. The overall rate of Ca(II) adsorption is likely to be controlled by the chemical process. The coordination mechanism of chitosan derivatives with Ca(II) was studied by infrared and X-ray photoelectron spectroscopy. The results indicated that –NH– of KCTS was coordinated. Nitrogen of amino, oxygens of hydroxamic acid, and carbonyl in HKCTS coordinated with Ca(II).

Keywords: Chitosan derivatives; Adsorption; Chelating reaction

1. Introduction

Chitosan, a biopolymer produced from chitin by partially deacetylating its acetamido groups with a strong alkaline solution, contains high contents of amino and hydroxyl functional groups. Different from most other natural polymers, chitosan has high reactivity and processability for its specific molecular structure and polycationic nature [1, 2]. Chitosan has been reported to have high potential for adsorption of metal ions [3, 4], dyes [5], and proteins [6]. Chitosan is a powerful chelating agent, which easily form complexes with transition metals and heavy metals.

The ability of chitosan and derivatives to chelate Cu^{2+}, Pb^{2+}, Hg^{2+}, Cr^{2+}, Mg^{2+}, Ca^{2+}, Zn^{2+}, $A1^{3+}$, and Mn^{2+} has been studied, suggesting the possibility of using these polymers in the removal of metal ions in waste and natural waters [7]. Most of these studies investigated possible uses of such sorbents to remove heavy metals. Heavy-metal-ion removal with the use of chitinous materials is widely reported [8–10],

---

*Corresponding author. Email: psxf06@yahoo.com.cn

Journal of Coordination Chemistry
ISSN 0095-8972 print/ISSN 1029-0389 online
DOI: 10.1080/00958972.2011.568615

but the potential offered by these materials is so high that it deserves continued research.

In this work, chitosan derivatives were used as adsorbents and the mechanism of adsorption of Ca(II) onto chitosan derivatives were studied. The adsorption isotherms were correlated by $\mathrm{d}c/\mathrm{d}t = -kc^n$. Infrared (IR) and X-ray photoelectron spectroscopy (XPS) techniques are used to identify the sites affected by metal sorption and the mechanism involved. This information will be useful for further applications in the sequestration or removal of metal ions in industrial processes.

2. Experimental

2.1. *Chemicals*

Chitosan (CTS, MW4.9x105, degree of deacetylation: 95%) was procured from Dalian Xindie Chitin Co., Ltd. Theophylline was provided by Qingdao Medicine Institute. Alpha-ketoglutaric acid was purchased from Qianshan Science and Technology Development Company, Zhuhai, China. The other reagents were of analytical grade and used without purification. All solutions were prepared with deionized water.

2.2. *Preparation of KCTS and HKCTS*

KCTS and HKCTS were prepared as described in [11]. CTS (4.5 g) was swelling in deionized water (100 mL) and then alpha-ketoglutaric acid (7.2 g) was added. The pH of the solution was adjusted to 4.5–5.0 using sodium hydroxide solution. Then, sodium hydroxide was added to the stirred mixture. The pH of the polymeric solution was adjusted to 6.5–7.0 using hydrochloric acid solution and the reaction was further stirred for 24 h. The reaction was terminated by 95% alcohol and the precipitated polymer was filtered, washed 3–4 times with ethanol and diethyl ether. The generated polymer (KCTS) was purified in a Soxhlet extractor with ethanol and dried in an IR drier.

KCTS (4.5 g) was dissolved in water (100 mL) and the pH of the polymeric solution was adjusted to 4.0–4.5 using hydrochloric acid solution (1.0 N). Then, dicyclohexylcarbodiimide (DCCI, 0.74 g) was added to the stirred mixture. Two hours later, hydroxylamine hydrochloride (4.5 g) was added and the reaction was further stirred for 1 h, the pH of the reaction was raised to 6.0 using sodium hydroxide solution (1.0 N), and the mixture was stirred for 2 h. Thereafter, the pH was raised again to 9.0 and the reaction mixture was stirred for 24 h at room temperature. The reaction was terminated by precipitation with concentrated hydrochloric acid (20 mL) and acetone (200 mL). The precipitated polymer was filtered, washed 3–4 times with ethanol, followed by acetone and diethyl ether, respectively. The generated polymer (HKCTS) was purified in a Soxhlet extractor with ethanol and acetone, and dried at 60°C for 4 h.

2.3. *Characterization*

The FT-IR spectra were obtained in KBr disks on a Hitachi 270-50 FT-IR Spectrophotometer. XPS was used to determine the surface composition and chemical environment of metal-coordination compounds with chitosan derivatives. The XPS measurements were made on a VG ESCALAB MKII spectrometer with an Al-Kα X-ray source (1486.6 eV photons).

2.4. *Batch adsorption experiments*

Batch adsorption experiments were conducted by placing 0.5 g of the chitosan derivatives in a 100 mL flask with 50 mL calcium chloride solution of a known initial concentration. The mixture in the flask was shaken at room temperature on an orbit shaker operated at 100 rpm for 100 min or until adsorption equilibrium was established. The initial pH of the solutions was adjusted with NaOH to a desired value. The Ca(II) concentration in solutions were determined spectrophotometrically by taking and analyzing solution samples periodically. The adsorbed amount of Ca(II) per unit weight of chitosan derivatives at time t, $Q(t)$ ($\mathrm{mg\,g^{-1}}$) was calculated from the mass balance equation as follows:

$$Q(t) = \frac{(C_0 - C_t)V}{m} \tag{1}$$

where C_0 and C_t ($\mathrm{mg\,L^{-1}}$) are the initial Ca(II) concentration and the Ca(II) concentrations at any time t, respectively, V is the volume of the Ca(II) solution, and m is the weight of the chitosan derivatives.

3. Results and discussion

Figure 1 shows a schematic representation of the preparation of KCTS and HKCTS.

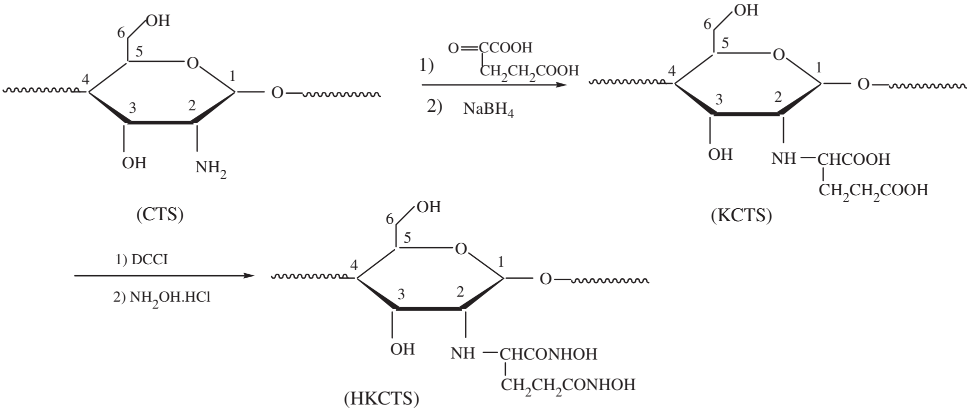

Figure 1. Synthetic route for KCTS and HKCTS.

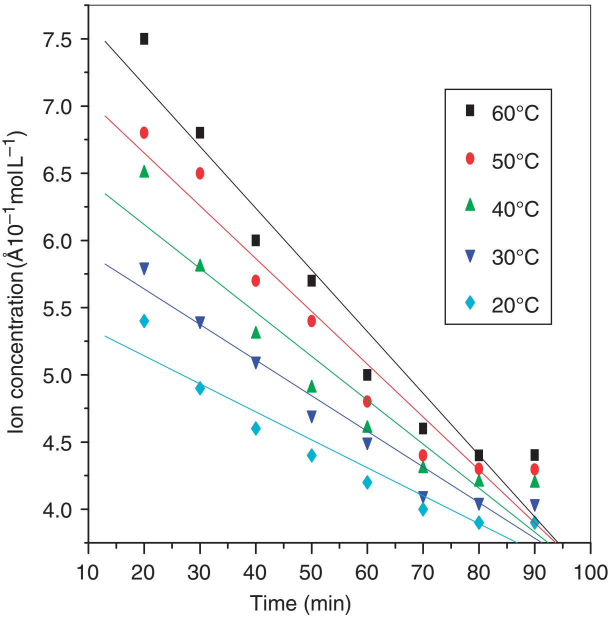

Figure 2. Plot of the pseudo second-order equation of KCTS.

3.1. *Effect of ion concentration on Ca adsorption*

Figures 2 and 3 show the change in ion concentration with time for chelating reaction between KCTS and HKCTS with Ca(II) at 20°C, 30°C, 40°C, 50°C, and 60°C. Adsorption is mainly chemical-chelating adsorption. The results indicate that the adsorption rate increases with increasing temperature and shows the adsorbing rates for Ca(II) on HKCTS are significantly higher than those on KCTS.

3.2. *The kinetics of chelation*

To investigate the mechanism of adsorption processes such as mass transfer and chemical reaction, the experimental data in figures 2 and 3 were fitted by linear correlation in graphs of $\ln c$ *versus* t, $-2/\sqrt{c}$ *versus* t, and $1/c$ *versus* t. The fitting results are listed in tables 1 and 2. Based on the correlation coefficients, the shapes of the isotherm curves were similar to the kinetic function of $1/c = kt$ and the rate equation for chelation between chitosan derivatives with Ca(II) was $\mathrm{d}c/\mathrm{d}t = -kc^2$. The data correlated well with the second-order kinetic model; similar results about the chelating reaction process were reported by Wu *et al.* [12] on adsorption of Cu^{2+} onto chitosan in the presence of complexing agents. The adsorption of Hg^{2+}, Cu^{2+}, and Ni^{2+} by modified chitosan magnetic resin in the study carried out by Zhou *et al.* [13] was also best described by the second-order model, in agreement with the kinetic results found in our study for adsorption of Ca(II) onto chitosan derivatives.

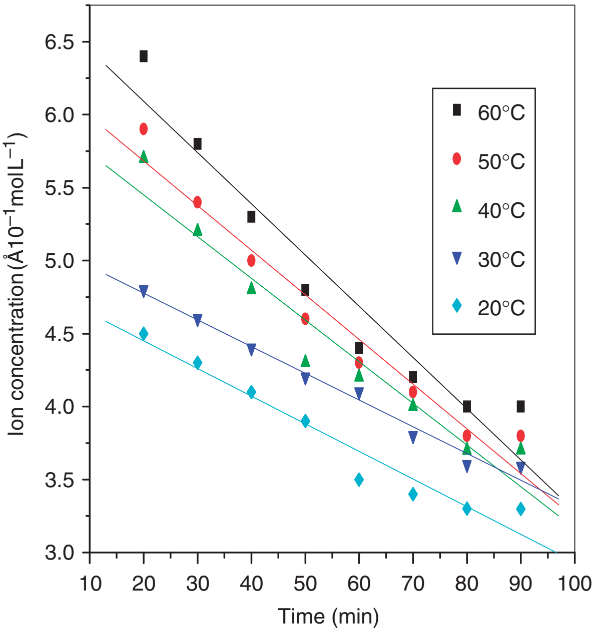

Figure 3. Plot of the pseudo second-order equation of HKCTS.

Table 1. ln*c*–*t*, $-2/\sqrt{c}$–*t*, 1/*c*–*t* fitting results of KCTS.

	ln*c*–*t*		$-2/\sqrt{c}$–*t*		1/*c*–*t*	
T (°C)	*k*	*r*	*k*	*r*	*k*	*r*
20	0.00526	0.9741	0.2452	0.9856	11.651	0.9913
30	0.00626	0.9628	0.2861	0.9633	13.109	0.9932
40	0.00658	0.9380	0.3212	0.9702	14.347	0.9932
50	0.00831	0.9403	0.3613	0.9912	15.579	0.9908
60	0.00996	0.9506	0.4048	0.9502	16.882	0.9928

Table 2. ln*c*–*t*, $-2/\sqrt{c}$–*t*, 1/*c*–*t* fitting results of HKCTS.

	ln*c*–*t*		$-2/\sqrt{c}$–*t*		1/*c*–*t*	
T (°C)	*k*	*r*	*k*	*r*	*k*	*r*
20	0.00470	0.96808	0.2212	0.9732	13.304	0.9970
30	0.00556	0.95368	0.2942	0.9861	14.548	0.9932
40	0.00697	0.98699	0.3204	0.9883	15.343	0.9922
50	0.00833	0.93575	0.3328	0.9684	16.492	0.9990
60	0.00965	0.94562	0.3518	0.9456	17.532	0.9967

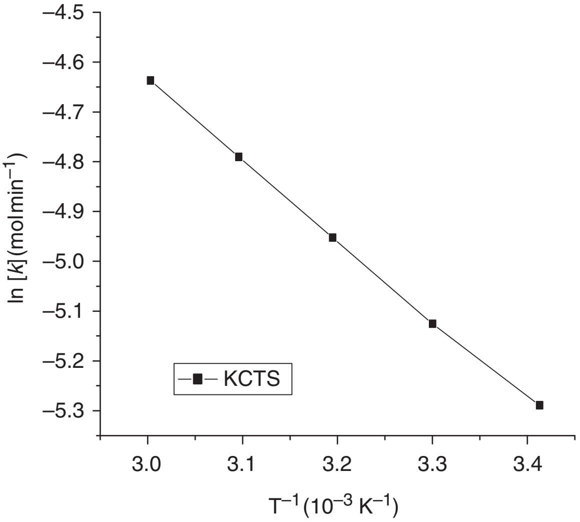

Figure 4. Relationship between ln$k$ and $1/T$ (KCTS).

The rate constant k at different temperatures listed in tables 1 and 2 were then used to estimate the activation energy of the adsorption of Ca(II) onto KCTS and HKCTS by the Arrhenius equation [14, 15]:

$$\ln \kappa = \ln A - \frac{E_a}{RT} \tag{2}$$

where E_a, R, and A refer to the Arrhenius activation energy, the gas constant, and the Arrhenius factor, respectively. To extract A and E_a, we plot the series of rate constants measured at different temperatures in graphs of ln$k$ *versus* $1/T$. As shown in figures 4 and 5, the corresponding activation energy was determined from the slope of the linear plot. Values of the activation energy were 13.31 ± 0.01 and $14.76 \pm 0.01\,\mathrm{kJ\,mol^{-1}}$, respectively. Riemam and Walton [16] reported that the activation energy range of chelating reactions was 8–16 $\mathrm{kJ\,mol^{-1}}$. A similar result about the chelating reaction process was reported by Oguz [17]. The relatively low activation energy indicates that adsorption of Ca(II) easily takes place by KCTS and HKCTS. It is likely that the whole chelating process is in agreement with the chemisorption mechanism being a rate-controlling mechanism [18].

3.3. *Mechanism of chelating reaction chitosan derivatives with Ca(II)*

3.3.1. FT-IR analysis. Complexation of amide groups to Ca(II), within KCTS–Ca, can be satisfactorily illustrated by IR spectroscopy, as shown in figure 6. The spectrum of KCTS–Ca polymeric matrix shows principal complex absorption bands at $1580\,\mathrm{cm^{-1}}$; in contrast, the IR spectrum of KCTS shows an amide carbonyl band at $1650\,\mathrm{cm^{-1}}$. Accordingly, one can conclude that amide carbonyls were shifted to lower

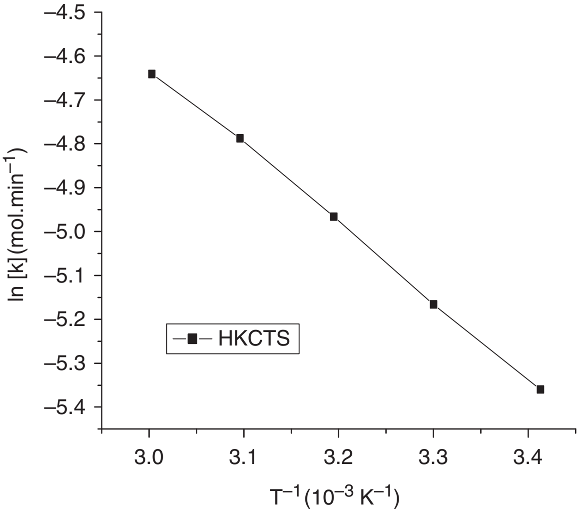

Figure 5. Relationship between ln$k$ and $1/T$ (HKCTS).

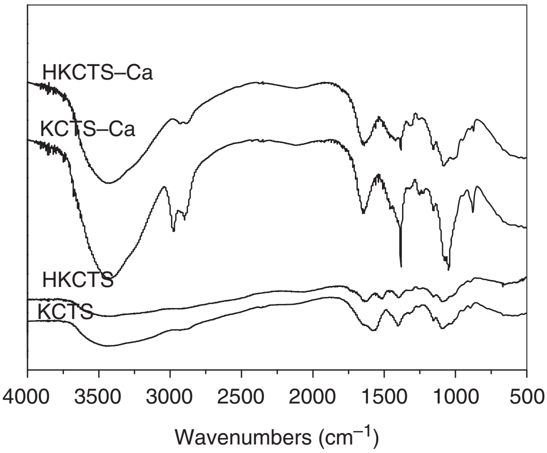

Figure 6. IR spectra of KCTS, HKCTS, KCTS–Ca, and HKCTS–Ca.

frequencies upon complexation to calcium, that is, from 1650 to 1580 cm^{-1} for amide carbonyls. Such a shift indicates that amide groups take part in chelation.

IR spectroscopy was also used to probe the structure of HKCTS–Ca. The IR spectrum of HKCTS–Ca polymeric matrix (figure 6) shows both carboxyl and amide carbonyls shifted to lower frequencies upon complexation to calcium, that is, from 1655 to 1560 cm^{-1} for amide carbonyls and from 1734 to 1665 cm^{-1} for carboxylic carbonyls; the formed hydroxamic carbonyl groups at 1636 cm^{-1} in HKCTS–Ca were also shifted to lower frequencies upon complexation with calcium. Such shifts indicate that hydroxyl in hydroxylamine, carboxyl, and amide are coordinated to calcium, suggesting

Table 3. Binding energy data (eV).

Sample	C1s	O1s	N1s	$Ca^{2+}2p_{3/2}$
KCTS	284.7	531.6	398.8	–
KCTS–Ca	284.7	531.6	398.8, 399.6	348.3, 346.6
HKCTS	284.7	531.7	398.7	–
HKCTS–Ca	284.7	531.7, 532.1	398.7, 399.8	348.3, 345.8

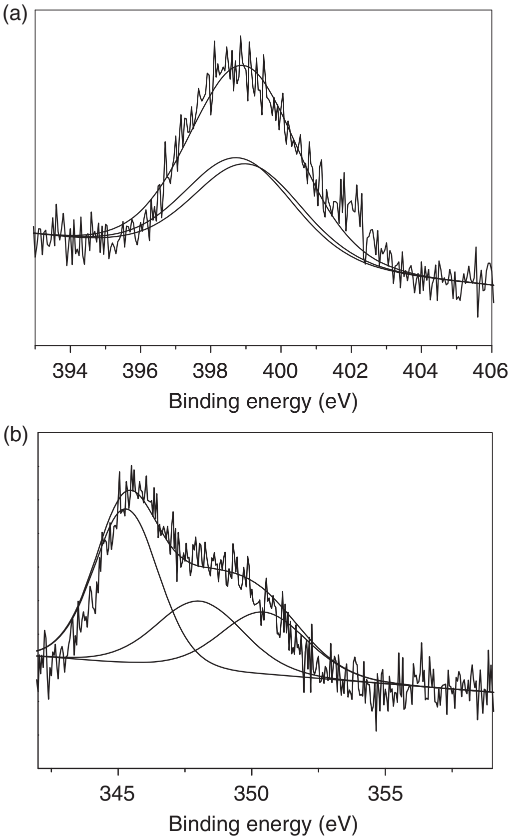

Figure 7. XPS spectra of N1s(a) and Ca^{2+}2p3/2(b) of KCTS–Ca.

that interaction between HKCTS/KCTS and calcium ion is mainly the chemical adsorption not physical adsorption.

3.3.2. XPS analysis. The XPS binding energies obtained from the C1s, O1s, N1s, $Ca^{2+}2p_{3/2}$ core levels of the diazine complexes are listed in table 3.

The C1s XPS spectra did not show significant changes of the C1s BEs before and after Ca adsorption (less than 0.5 eV) (table 3). Since both FT-IR and XPS spectra could not provide clear evidence that the chemical bonds associated with the carbons

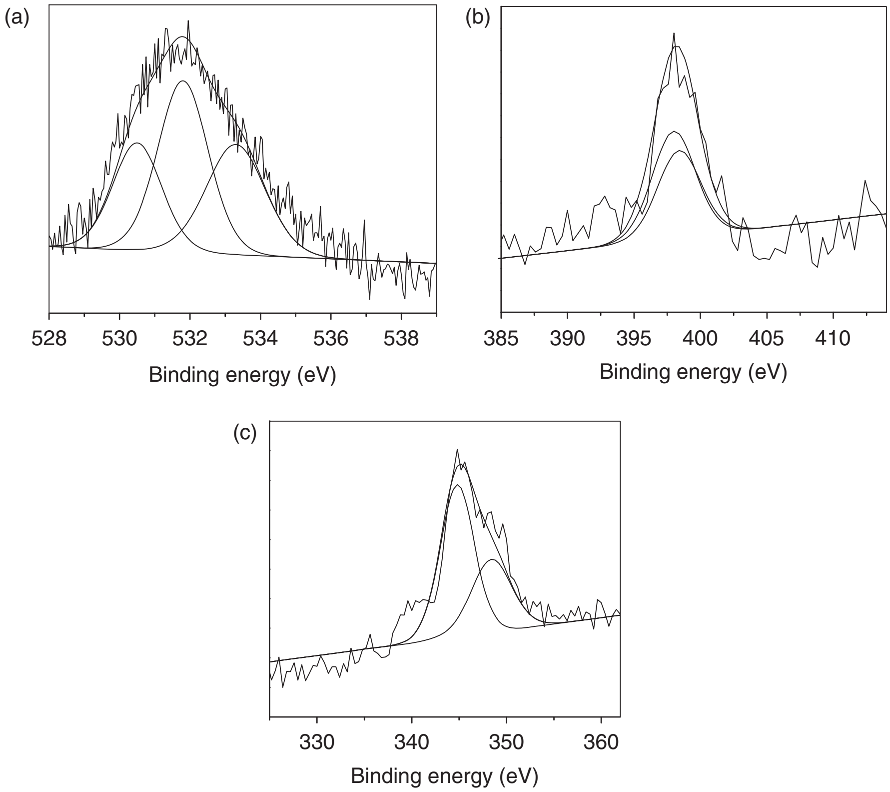

Figure 8. XPS spectra of O1s(a), N1s(b), and $Ca^{2+}2p_{3/2}$(c) of HKCTS–Ca.

on both beads were significantly changed after Ca adsorption, it may be speculated that the contribution of Ca–carbon interaction to Ca adsorption on the beads was mainly through a non-specific interaction (physical adsorption, electrostatic attraction, etc.) or a very weak chemical interaction. Therefore, carbon does not take part in complexation.

Figures 7(b) and 8(c) show the typical XPS wide scan spectra for chitosan derivatives before and after Ca adsorption. It is clear that a new peak at BE of 346.6 eV for KCTS or 345.8 eV for HKCTS appear after Ca adsorption. The presence of a satellite band is representative of the oxidation state +2 for the Ca $2p_{3/2}$ orbital. Therefore, the peak at BE of 346.6 eV for KCTS or 345.8 eV for HKCTS provides evidence of Ca^{2+} being adsorbed on the surface of KCTS and HKCTS.

The O1*s* XPS spectra of KCTS, however, did not clearly show significant changes of the O1*s* BEs before and after Ca adsorption (less than 0.5 eV) (table 3). Therefore, oxygen does not take part in complexation. The O1*s* spectrum of HKCTS could be decomposed into two single peaks (figure 8a) with assignments of 531.7 eV as carboxyl oxygen (–CO–O–), and 532.1 eV as methylene bound to one oxygen ($–CH_2–O–$). This indicates that oxygen in carboxyl of HKCTS coordinate, which is in agreement with the FT-IR findings.

In figures 7(a) and 8(b), the typical N1s XPS spectra of KCTS and HKCTS before and after Ca adsorption are presented. Before Ca adsorption, there is only one peak

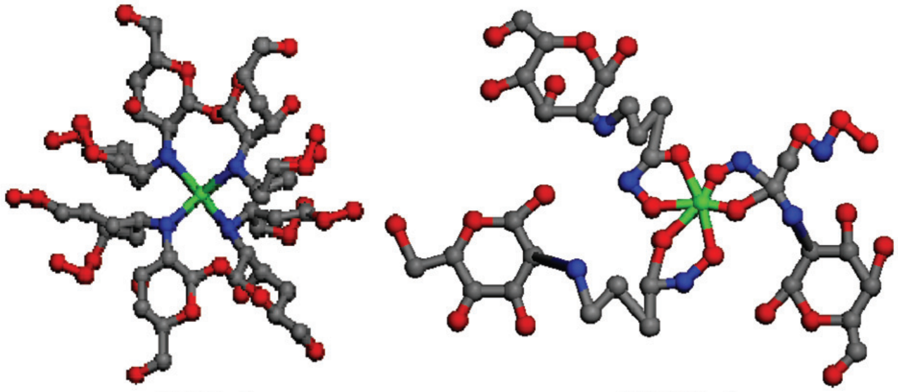

KCTS–Ca HKCTS–Ca

Figure 9. Possible structures of KCTS–Ca and HKCTS–Ca:●(N)●(C)● (O) ● (Ca).

at 398.8 eV for KCTS or at 398.7 eV for HKCTS, attributed to nitrogen in –NH_2 and/or –NH– on the surfaces of KCTS and HKCTS. After Ca adsorption, a new peak at BE of 399.6 eV for KCTS or at BE of 399.8 eV for HKCTS is observed, indicating that some nitrogens existed in a more oxidized state on the beads' surfaces due to Ca adsorption. This phenomenon can be attributed to the formation of $R–NH_2Ca^{2+}$, in which a lone pair of electrons on nitrogen was donated to Ca^{2+}, and, as a consequence, the electron density of nitrogen was reduced, resulting in a higher BE peak observed. Therefore, the XPS spectra provide evidence of Ca binding to nitrogens, in agreement with the FT-IR findings.

Based on the analysis above, we speculate the molecular structure of chitosan-derivative–metal complexes (figure 9).

4. Conclusions

In this study, the adsorption isotherms were correlated by $dc/dt = -kc^n$. By means of linear correlation, the shapes of the isotherm curves were similar to the kinetic function of $1/c = kt$ and the rate equation was $dc/dt = -kc^2$. This suggests that the rate-limiting step may be the chemical adsorption not mass transport. The mechanisms of chelating reaction between chitosan derivatives and Ca(II) are investigated by IR spectral analysis and X-ray photoelectron spectroscopy analysis. The results predict that these chitosan derivatives will have wide-ranging applications in the sequestration or removal of metal ions in industrial processes.

Acknowledgments

This work was supported by research grants from the National Science Foundation of China (Project No. 20576142), the Postdoctoral research fund of China (No. 20090461026), and the education subject of Hunan province of China (No. 10C0178).

References

[1] M.N.V. Ravi Kumar. *React. Funct. Polym.*, **46**, 1 (2000).
[2] Y. Sag, Y. Aktay. *Biochem. Eng. J.*, **12**, 143 (2002).
[3] E. Guibal, C. Milot, J.M. Tobin. *Ind. Eng. Chem. Res.*, **37**, 1454 (1998).
[4] W.S.W. Ngah, S.A. Ghani, L.L. Hoon. *J. Chin. Chem. Soc.*, **49**, 625 (2002).
[5] M.S. Chiou, H.Y. Li. *J. Hazard. Mater. B*, **93**, 233 (2002).
[6] X.F. Zeng, E. Ruckenstein. *J. Membr. Sci.*, **148**, 195 (1998).
[7] L. Furlan, V.T. de Fávere, M.C.M. Laranjeira. *Polymer*, **37**, 843 (1996).
[8] E. Guibal. *Sep. Purif. Technol.*, **38**, 43 (2004).
[9] A.J. Varma, S.V. Deshpande, J.F. Kennedy. *Carbohydr. Polym.*, **55**, 77 (2004).
[10] B. Krajewska. *Enzyme Microb. Technol.*, **35**, 126 (2004).
[11] P. Ding, K.-L. Huang, G.-Y. Li, Y.-F. Liu, W.-W. Zeng. *Int. J. Biol. Macromol.*, **39**, 222 (2006).
[12] F.C. Wu, R.L. Tseng, R.S. Juang. *Water Res.*, **35**, 613 (2001).
[13] L. Zhou, Y. Wang, Z. Liu, Q. Huang. *J. Hazard. Mater.*, **161**, 995 (2009).
[14] M. Dogan, M. Alkan. *Chemosphere*, **50**, 517 (2003).
[15] M. Chairat, S. Rattanaphani, J.B. Bremner, V. Rattanaphani. *Dyes Pigm.*, **64**, 231 (2005).
[16] W. Riemam, H. Walton. *International Series of Monographs in Analytical Chemistry*, Pergamon Press, Oxford (1970).
[17] E. Oguz. *Colloids Surf., A*, **295**, 258 (2007).
[18] M.S. Chiou, P.Y. Ho, H.Y. Li. *Dyes Pigm.*, **60**, 69 (2004).